International Journal of Chronic Obstructive Pulmonary Disease

Dovepress
Taylor & Francis Group

Open Access Full Text Article

ORIGINAL RESEARCH

Identification of Dendritic Cell-Associated Genes in COPD Based on Bioinformatics

Zengyu Huo, Jiawei Zou, Siyi Ou, Cunlai Xu, Linlin Xiao, Feng Chen, Yang Yang, Siming Chen, Xiangyuan Cen, Yirao Qin, Jing Bai

Department of Respiratory and Critical Care Medicine, The First Affiliated Hospital of Guangxi Medical University, Nanning, Guangxi, People's Republic of China

Correspondence: Jing Bai, Department of Respiratory and Critical Care Medicine, The First Affiliated Hospital of Guangxi Medical University, Nanning, Guangxi, People's Republic of China, Email Bj1312005@sr.gxmu.edu.cn

Background: The activation of dendritic cells, which is atypical, is vital for triggering the acquired immune response in people afflicted with chronic obstructive pulmonary disease (COPD). This research seeks to pinpoint significant genes linked to dendritic cells within the lung tissues of COPD patients by utilizing bioinformatics predictions and experimental validation.

Methods: Differentially expressed genes of classical dendritic cells (cDCs) were identified using single-cell RNA sequencing (scRNA-seq) data from GSE196638, and their biological functions and regulatory signaling pathways were thoroughly explored. Additionally, RNA sequencing (RNA-seq) data from GSE26296 was utilized to analyze differentially expressed genes in myeloid dendritic cells (mDCs) of emphysema patients. The RNA-seq data from GSE38974 underwent weighted gene co-expression network analysis (WGCNA) along with differential analysis to pinpoint genes that are differentially expressed and modules linked to COPD. Validation was performed using a mouse model of emphysema induced by cigarette smoke (CS) and bone marrow-derived dendritic cells (BMDCs) exposed to 3% cigarette smoke extract (CSE).

Results: The genes that showed differential expression in cDCs and mDCs were mainly associated with immune responses, the reaction to interferon-gamma, the differentiation of Th1 and Th2 cells, along with the signaling pathways of TNF and IL-17. The WGCNA results revealed that the green-yellow and red modules exhibited the highest correlation coefficients with the COPD phenotype. An assessment of the genes that are expressed differently between cDCs and mDCs, combined with the intersection of GSE38974 module genes and differentially expressed genes, results in the identification of four dendritic cells (DCs)-related genes: one upregulated signature gene (RASGRP3) and three downregulated signature genes (C1QB, BLOC1S2, VSIG4). In both the lung tissues of mice with CS-induced emphysema and in CSE-treated BMDCs, RT-qPCR validated the expression trends of these four genes. Concomitantly, Western blot revealed a reduction in VSIG4 protein level in the lung tissues of emphysema mice compared with the control group.

Conclusion: RASGRP3, C1QB, BLOC1S2, and VSIG4 may represent DCs-related genes in the lung tissue of COPD patients, potentially involved in the development and progression of emphysema.

Keywords: chronic obstructive pulmonary disease, bioinformatics, dendritic cells, immune microenvironment

Introduction

Chronic obstructive pulmonary disease (COPD) is a significant respiratory condition that is primarily marked by persistent inflammation of the airways. This inflammation leads to a gradual narrowing of the air passages, which can severely impact an individual's ability to breathe. The chronic nature of this disease means that the inflammation does not resolve over time, resulting in long-term respiratory issues that can significantly affect a person's quality of life. The intricate regulatory network involving various inflammatory mediators and immune cells adds to the complexity and multiplicity of its pathogenesis.[1] Smoking and air pollution are the primary contributing factors to COPD, activating immune cells in the lungs and triggering a sustained immune response, which includes the infiltration and abnormal activation of dendritic cells.[2–4] The rates of incidence and mortality associated with COPD are on the rise, leading to

Received: 20 June 2025
Accepted: 2 October 2025
Published: 29 October 2025

serious consequences for patients and considerable financial strains. Therefore, the discovery of new potential target genes is crucial for advancing research into the pathogenesis and treatment of COPD.[5,6]

Dendritic cells (DCs), as one of the core antigen-presenting cell populations in the immune system, have garnered significant attention due to their exceptional capabilities in antigen capture, processing, and presentation. They are indispensable for initiating and managing immune responses throughout the body.[7,8] DCs can be classified into two main types: conventional dendritic cells (cDCs) and plasmacytoid dendritic cells (pDCs). Within the category of cDCs, two main subsets can be identified: CD103+ cDC1s and CD11b+ cDC2s. In humans, myeloid dendritic cells (mDCs) are mainly associated with cDC2s, express myeloid markers, and are essential for T-cell activation.[9] Recent research showed a strong connection between the pathophysiological mechanisms of COPD and the functional status of DCs, with their involvement substantiated by multiple experimental data. Through interactions with various immune cells, DCs modulate inflammatory responses and immune reactions, thereby influencing the progression of COPD.[10–12] Cigarette smoke (CS) exposure can induce an abnormal distribution of dendritic cell subsets within lung tissue. Following their migration to inflammatory regions, these cells interact with CD4+ T lymphocytes, triggering dysregulation of immune homeostasis between Th1/Th17 cells and regulatory T cells (Tregs). This dysregulation ultimately drives the inflammatory cascade and pathological progression of COPD.[13–16] In the lung tissue of individuals suffering from COPD, there is notable proliferation observed in the CD8+ T cell subset. In this disease, DCs trigger an overactivation of CD8+ T cells and facilitate their transformation into cytotoxic T cells by means of antigen presentation and the overexpression of pro-inflammatory co-stimulatory molecules. Research has shown that CD8+ T cells can induce programmed cell death during the progression of COPD, a process that directly contributes to lung parenchymal injury and exacerbates the inflammatory response.[17–19] In the pathological process of COPD, chemokines such as CXCL3 and CXCL2, secreted by dendritic cells, play a significant role. These chemokines promote inflammatory changes in lung tissue by mediating the migration of neutrophils and lymphocytes.[20,21] Our earlier studies have demonstrated that exposure to CS significantly elevates the IL-27 expression in DCs within the lung tissues of emphysema model mice. This effect has similarly been noted in bone marrow-derived dendritic cells (BMDCs) induced by cigarette smoke extract (CSE). The study indicates that IL-27, recognized as an important cytokine, promotes the differentiation of IFN-γ-positive CD8+ T cells into the Tc1 subset. This subset is essential in the inflammatory pathological processes associated with COPD, resulting in persistent and uncontrolled inflammatory reactions.[22] Although existing research has identified several genes related to dendritic cells in COPD, further exploration and elucidation are necessary.

Single-cell RNA sequencing (scRNA-seq) technology has yielded breakthroughs in understanding the mechanisms underlying inflammatory and autoimmune diseases. Certain studies have employed this approach to uncover previously unknown genes and signaling pathways associated with DCs in inflammatory and autoimmune diseases.[23–25] Consequently, our study aims to investigate dendritic cell-related genes in COPD through bioinformatics analysis and experimental validation. We utilized scRNA-seq data from GSE196638 to examine the functional differences of cDCs in lung tissues between control groups and patients with COPD, identifying differentially expressed genes. Concurrently, we screened for differentially expressed genes in mDCs using RNA-seq data from GSE26296. Additionally, we integrated COPD-related module genes and differentially expressed genes from GSE38974. By analysing the data collected, we pinpointed specific genes related to DCs that are linked to COPD. We then quantified these genes by RT-qPCR in lungs of CS-induced emphysema mice and CSE-treated BMDCs, and assessed VSIG4 protein in emphysematous lung tissue. This study offers a thorough perspective by pinpointing genes that show significant differential expression in the lung tissues of patients with COPD, as well as in cDCs within the lung tissues, and in mDCs in the lung tissues of emphysema patients. By examining these distinct subsets, the research uncovers crucial dendritic cell genes involved in the progression of COPD. Furthermore, this investigation provides valuable insights that could inform the future development of innovative immunotherapeutic approaches for COPD treatment.

Methods

Data Source

The data employed in this research were sourced from the publicly accessible genomic data repository known as Gene Expression Omnibus. This repository, which can be found at the website http://www.ncbi.nlm.nih.gov/geo, serves as

a comprehensive platform for the storage and sharing of genomic expression data. Specifically, three independent sequencing datasets were integrated: the scRNA-seq dataset (GSE196638) comprises lung tissue samples from three controls and three COPD patients, providing foundational data for gene expression analysis. Meanwhile, the RNA-seq dataset (GSE26296) includes samples of mDCs isolated from the lung tissues of three controls and three emphysema patients. Additionally, the RNA-seq dataset (GSE38974) offers a larger sample size, comprising nine control samples and eighteen COPD patient lung tissue samples. All human datasets (GSE196638, GSE26296 and GSE38974) are publicly available and de-identified. The Medical Ethics Committee of the First Affiliated Hospital of Guangxi Medical University formally reviewed and approved this research (Approval No. 2025-E0752) in accordance with the Declaration of Helsinki and institutional guidelines for secondary use of human data.

Single-Cell Sequencing Data Analysis

A systematic quality control screening was conducted on all samples from the GSE196638 dataset. The screening criteria included retaining samples with total gene counts ranging from 300 to 5000, mitochondrial gene expression proportion <10%, erythrocyte gene expression proportion <3%, and total unique molecular identifier (UMI) counts >1000.[26] After conducting quality control, we kept 18,646 cells within the control group and 26,958 cells in the COPD group. Subsequently, we standardized the expression matrix of the higher-quality cells, identified and adjusted for batch effects, and combined the six samples utilizing the Harmony algorithm. By invoking the three functional modules "FindNeighbors", "FindClusters", and "RunUMAP", we set the resolution to 0.6 to categorize the cells into distinct clusters. Ultimately, we labeled the clusters of cells using established marker genes associated with specific cell types. The "FindAllMarkers" function was employed to analyze the cDCs clusters in both the COPD and control groups, identifying significantly differentially expressed genes with log2fc $\geq$ 0.26 and P-value < 0.05. To further elucidate the functional traits of the genes that are expressed differently, the analysis toolkit known as "clusterProfiler" was employed to perform functional annotation and pathway enrichment analyses through Gene Ontology (GO) and the Kyoto Encyclopedia of Genes and Genomes (KEGG). Furthermore, to investigate the functional traits of these genes, gene set enrichment analysis (GSEA) was carried out utilizing gene sets sourced from the Molecular Signatures Database (MsigDB) to assess the enrichment of gene sets at both ends of the ranked gene list. The Seurat object was then converted to a CellDataSet object in Monocle, where dimensionality reduction of cells was achieved through the DDRTree method, followed by pseudotime analysis with the Monocle package to infer developmental trajectories. Additionally, the CellChat package was utilized for cell communication analysis, which facilitated the identification of intercellular interactions and the visualization of the cell communication network.[27–30]

Differential Expression Gene Analysis and Functional Enrichment in the GSE26296 Dataset

Differential expression analysis was conducted on the expression matrix of mDC samples isolated from lung tissues of controls (n = 3) and emphysema patients (n = 3) in the GSE26296 dataset using the limma package. The significance threshold was set at $p < 0.05$ and $|\log2(\text{fold change, FC})| > 0.5$. To clarify the functional traits of the genes that are expressed differently, analyses of GO and KEGG were conducted. GO analysis was used to thoroughly examine the possible functions of the genes that were expressed differently in terms of cellular structure, molecular activities, and biological processes. The KEGG analysis emphasized the specific enrichment characteristics of these genes in metabolic pathways and signal transduction networks.[31–34]

GSE38974 Dataset WGCNA and Differential Expression Analysis

This study involved examining the GSE38974 dataset through weighted gene co-expression network analysis (WGCNA) to create gene modules that display comparable expression patterns.[35,36] To begin with, a scale-free network was constructed by identifying a suitable soft threshold. The hierarchical clustering algorithm was then applied to group genes exhibiting high co-expression into the same module. Subsequently, the "blockwiseModules" function was utilized to identify gene modules, while the "cor" function calculated the correlation between each module and COPD, thereby identifying gene modules

significantly associated with COPD. To delve deeper into gene functionality, an analysis of differential expression was performed, establishing a significance threshold of $p < 0.05$ and $|\log2(\text{fold change, FC})| > 0.5$ to pinpoint genes that are significantly differentially expressed. Following this, these genes underwent GO and KEGG analysis.

Identify Common Differentially Expressed Genes

This research offers an extensive analysis of differentially expressed genes (DEGs) found in multiple datasets, including GSE196638 cDCs, GSE26296 mDCs, GSE38974, and WGCNA module genes. By integrating the DEGs from each dataset and utilizing an intersection approach, we identified genes that exhibited significant differential expression across all datasets. To visually illustrate the overlap of DEGs among the various datasets, a Venn diagram was constructed. Furthermore, we performed a Receiver Operating Characteristic (ROC) analysis on the identified common DEGs in the GSE38974 dataset to evaluate their diagnostic potential.

CS-Induced Emphysema Mouse Model

C57BL/6 male mice, SPF-grade, aged 5 to 6 weeks and weighing approximately 14 ± 2 g, were sourced from the Animal Experiment Center of Guangxi Medical University for this study. Throughout the experiment, the subjects were maintained in a controlled environment with a 12-hour light/dark cycle and had unrestricted access to food and water. A randomized grouping strategy was employed, resulting in two cohorts, each consisting of 8 mice: a control group exposed to normal air and a treatment group subjected to CS. CS exposure was facilitated within a specially constructed smoke chamber, where exposure occurred four times daily, utilizing 5 cigarettes per session for 60 minutes, with a 30-minute pause between sessions to maintain a consistent smoke concentration ranging from 140–160 mg/m^3. This protocol was implemented five days per week over a period of 24 weeks. For the control group, the animals were kept in a distinct ventilated room where they inhaled clean, filtered air. Lung tissue samples were obtained 24 hours following the final exposure for further examination. The Experimental Animal Ethics Committee of Guangxi Medical University approved this study (No. 202503381), ensuring compliance with the institution's guidelines for animal welfare and usage. All procedures were conducted in accordance with the Guide for the Care and Use of Laboratory Animals, 8th ed. (2011, rev. 2023) and the ARRIVE 2.0 guidelines. Upon conclusion of the experiment, the mice were humanely euthanized via intraperitoneal injection of pentobarbital to alleviate potential distress.

Histology

The right lung tissue from the mice was preserved in a 4% paraformaldehyde solution. Sample preparation was then conducted using the standard paraffin embedding method, followed by hematoxylin and eosin (H &E) staining. During the examination, five microscopic fields were randomly selected from each tissue section. The morphological alterations of the alveolar structure were assessed by calculating the mean linear intercept (MLI), based on established techniques from the literature.[37] Image data were quantitatively analyzed using ImageJ software for processing and calculations.

Preparation of CSE

Based on the preparation methods described in previous literature reports.[38,39] Collect the smoke from five cigarettes using a bubble collection device and dissolve it in 5 mL of phosphate-buffered saline (PBS) to prepare the CSE solution. Assess the absorbance of the CSE at a wavelength of 320 nm with a NanoDrop 2000 spectrophotometer to ascertain its concentration. To obtain a sterile stock solution of CSE, filter the solution through a 0.22 μm microporous membrane for sterilization.

Marrow-Derived Dendritic Cell Inducement

In this study, we utilized normal, healthy mice aged 6 to 10 weeks. The upper end of the femur and the lower end of the ankle joint were severed while maintaining the integrity of the joint. The samples were then immersed in 75% alcohol for 5 minutes and washed three times with PBS. Subsequently, the tibia and femur were extracted, and the bones were flushed with RPMI 1640 containing 10% fetal bovine serum to isolate bone marrow cells. Following the lysis of red blood cells with a specific lysis buffer, the cells were then transferred to cell culture dishes for plating. To the culture

system, we added 20 ng/mL of recombinant mouse IL-4 and recombinant mouse GM-CSF (Peprotech). After 4 hours of plating, the medium was replaced, suspended cells were discarded, and adherent monocytes were retained. On the second and fifth days of the culture process, a half-medium change was performed. On day 7, BMDCs were collected and purified using Miltenyi CD11c MicroBeads UltraPure (130–125-835), followed by treatment with 3% CSE at the concentrations referenced from our previous studies.[22,40,41] All animal research followed the guidelines established by the Council for the Care and Use of Animal subjects.

Western Blot (WB)

While BLOC1S2 showed the highest AUC among the candidate genes, this research centeres on validating the protein expression of VSIG4. This selection is largely driven by the enrichment of VSIG4 in dendritic cells and macrophages, along with its essential function in regulating T-cells and mediating COPD-related inflammatory responses. To confirm the protein expression of VSIG4, total proteins were isolated from lung tissue with RIPA lysis buffer and subsequently quantified using the BCA assay. Then, 50 μg of the protein samples were resolved by SDS-PAGE, and the proteins were transferred to PVDF membranes through the wet transfer technique. After blocking the membranes with 5% skim milk at room temperature for one hour, they were incubated overnight at 4 °C with anti-VSIG4 antibody (1:500, Bioss, China, cat# bs-0479R) alongside the internal reference β-tubulin antibody (1:6000, Abways, China, cat# AB0039). The next day, the membranes received DyLight™ 800-conjugated goat anti-rabbit IgG (1:10,000, CST, USA, cat# 5151) for one hour at room temperature. β-tubulin acted as the internal reference for lung tissue. Ultimately, the protein bands underwent grayscale analysis through ImageJ software to evaluate the expression level of VSIG4 quantitatively.

RT-qPCR Experimental Validation

RNA was isolated from BMDCs with the use of TRIzol reagent (Invitrogen). To guarantee the accuracy of the following experiments, both the purity and concentration of the isolated RNA were assessed to verify the quality of the RNA samples. Qualified samples were then reverse-transcribed into cDNA using the Promega kit. During the amplification step, the PCR reaction was performed using the SYBR® Premix Ex Taq II kit from Takara. Primer design was based on the Primer-BLAST platform provided by the National Center for Biotechnology Information (NCBI), with the final synthesis conducted by Sangon Biotech (Shanghai). The specific primers used is listed in Table 1.

Statistical Analysis

The data analysis was performed utilising the R software (version 4.2.1) as well as the GraphPad Prism (version 8.0). A two-tailed Student's *t*-test was utilized to assess the variations between the two groups, with a significance threshold established at 0.05. A p-value that falls below this limit signifies statistically significant results.

Table 1 The Sequences of RT-PCR Primers

RASGRP3: forward (5'-GCAGAGCCATTACCCTGGTT-3')
Reverse (5'-CTGGGTGGCTTGACTAGTGG-3')
C1QB: forward (5'-CTGAGGACCATCAACAGCCC-3')
Reverse (5'-CGTTGCGTGGCTCATAGTTC-3')
BLOC1S2: forward (5'-ATGATTGAGGAGCAGGTGGC-3')
Reverse (5'-CATCGCTTCTCCAACTTCTTGTA-3')
VSIG4: forward (5'-AATGGCTGGTAAGACACGGC-3')
Reverse (5'-GTGCAGGGTTGTAGGTGCTT-3')
β-ACTIN: forward (5'-CTCGCTTCGGCAGCACATATACT-3')
Reverse (5'-ACGCTTCACGAATTTGCGTGTC-3')

Results

scRNA-Seq GSE196638 Identifies Dendritic Cells and Associated Genes

The process outlined in this study can be seen in Figure 1. Prior to analysis, we conducted quality control on the data, retaining cells with a total gene count exceeding 300 but below 5000, a mitochondrial gene expression rate under 10%, an erythrocyte gene expression rate below 3%, and a total of UMI counts greater than 1000 (Figure 2A). After normalizing the data, principal component analysis (PCA) was utilized to achieve initial dimensionality reduction, as illustrated in Figure 2B. The Harmony algorithm was utilized to integrate the six samples from the scRNA-seq GSE196638 dataset, with the UMAP clustering of the samples depicted in Figure 2C, which demonstrates effective sample clustering with high consistency. Following the processes of dimensionality reduction and clustering, the cells were grouped into 26 distinct clusters. Together with cell type classification, the expression levels of frequently used marker genes were utilized to annotate these clusters, leading to the identification

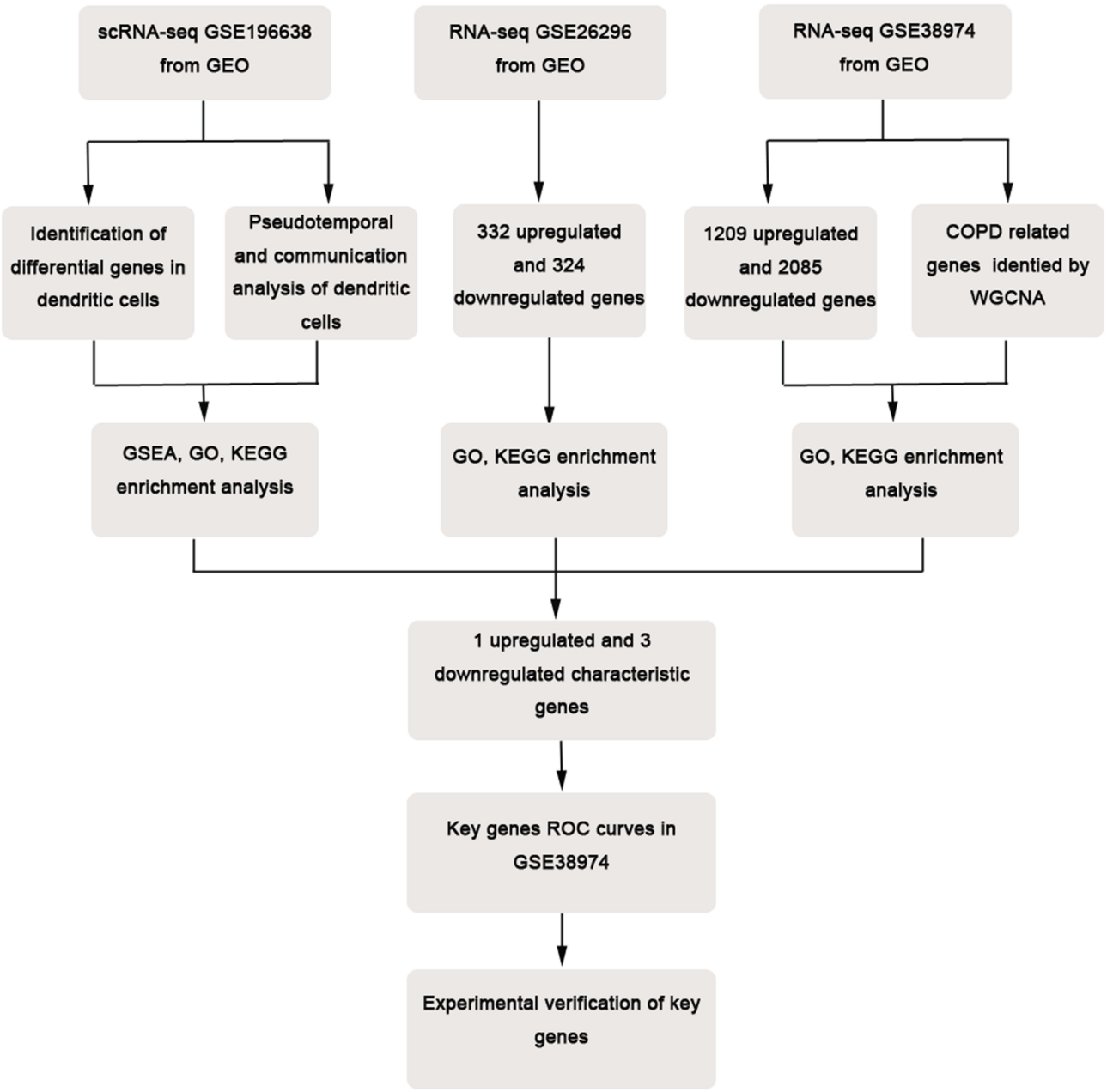

Figure 1 Flowchart of this study.

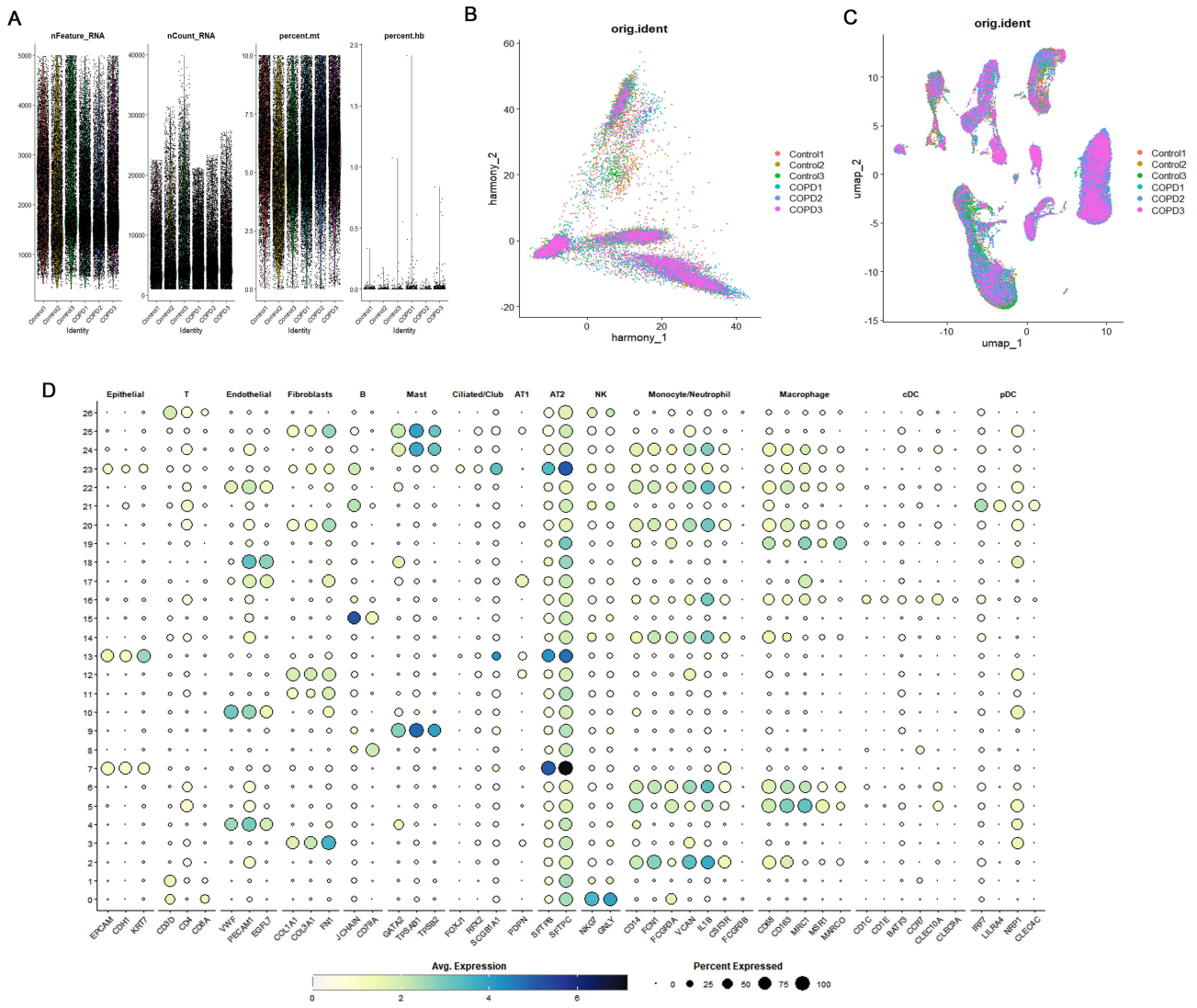

Figure 2 Dimensionality Reduction and Annotation of scRNA-seq GSE196638. (**A**) Quality control, adjusting the proportions of mitochondrial and erythrocyte genes. (**B**) PCA dimensionality reduction. (**C**) UMAP plot showing the distribution of 6 samples after batch effect removal. (**D**) Bubble plot depicting marker gene expression in control and COPD sample cells.

of 13 unique cell types: NK, T, Monocyte/Neutrophil, Fibroblasts, Endothelial, Macrophage, AT2, B, Mast, cDC, AT1, pDC, and Ciliated/Club (Figures 2D and 3A). Figure 3B depicts the distribution of various cell types within the two sample groups, with specific numerical data available in Table 2. In the COPD cohort, the levels of NK, T, B, cDC, and pDC were higher in comparison to the Control group, suggesting changes in the lung tissue microenvironment linked to the COPD disease state. We focused our analysis on cDCs, conducting a differential analysis that revealed a total of 2005 downregulated genes and 1184 upregulated genes (Figure 3C).

Enrichment Analysis and Pseudotime Analysis of cDCs

GO analysis for genes that are differentially expressed in cDCs indicated their main role in immune processes mediated by lymphocytes. The cellular components were predominantly enriched in the secretory granule lumen, cytoplasmic vesicle lumen, and vesicle lumen, indicating that these lineage cells possess robust secretory functions and are actively engaged in the formation and transport of secretory granules. During the analysis of molecular function enrichment, the associated genes predominantly showed enrichment in activities related to protein tyrosine/threonine phosphatases as well as MAP kinase tyrosine/serine/threonine phosphatases. This indicates that these genes could be vital in essential phosphorylation and dephosphorylation

https://doi.org/10.2147/COPD.S543753

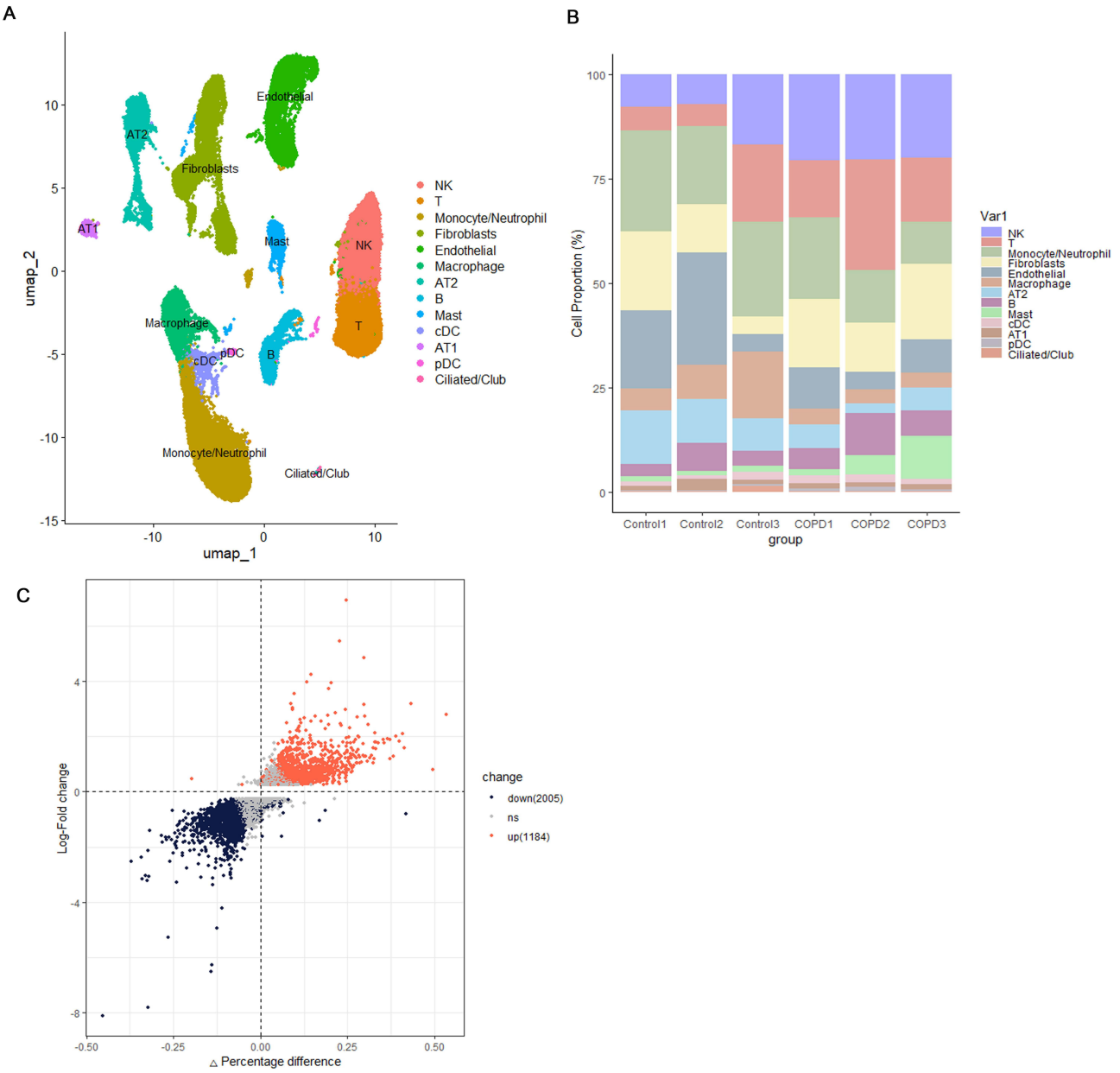

Figure 3 Single-cell landscape: Subpopulation composition, proportion and cDCs differential genes. (**A**) UMAP of 13 cell types in scRNA-seq GSE196638. (**B**) Calculation of the percentage of each cell type present in individual samples. (**C**) Volcano plot highlighting differentially expressed genes within cDCs.

processes occurring within the cell, thereby playing a role in cellular signal transduction and regulatory mechanisms (Figure 4A). The differentially expressed genes in cDCs are also primarily involved in KEGG enrichment analysis of coronavirus-COVID-19, apoptosis, Th1 and Th2 cell differentiation, and the NOD-like receptor signaling pathway. cDCs may play a role in the progression of COPD through their regulation of T cell differentiation and apoptosis, and activation of inflammatory pathways (Figure 4B). Following this, we assessed the gene set enrichment scores for cDCs using the marker gene sets sourced from the MsigDB database (Figure 4C). In summary, the gene sets associated with cytokine-cytokine receptor interactions and the differentiation of Th17 cells were identified as being enriched in cDCs. To gain a deeper understanding of the developmental trajectory of cDCs under disease conditions, we conducted a pseudotime analysis on these cells. The results indicated the presence of a node in the myeloid developmental trajectory of the Control group (Figure 5A and B), where cDCs were observed in the early developmental stage. In contrast, the COPD samples exhibited three nodes, with cDCs appearing in the early

Table 2 Proportions of Various Cell Types Within Both the Control and the COPD Group

Cell Type	Control	COPD
NK	10.59308962	20.25169438
T	9.741410774	18.52657839
Monocyte/Neutrophil	21.88007757	14.1295389
Fibroblasts	11.61558072	15.42500326
Endothelial	16.54627599	7.339893508
Macrophage	9.784331818	3.614908733
AT2	10.43429119	4.505319094
B	4.443744389	7.030157823
Mast	1.211682766	5.510000744
cDC	1.257366662	1.620549615
AT1	1.67269116	1.266266281
pDC	0.188358618	0.709753844
Ciliated/Club	0.631098728	0.070335427

developmental stage; however, a concentration of cDCs and pDCs was noted in the late developmental stage (Figure 5C and D), a phenomenon that was not observed in the Control group samples.

Interpretation of the Biological Functions of cDCs

DCs influence various immune cells through intercellular interactions to exert biological functions involved in the COPD disease process. In the control group samples, cDCs primarily interact with AT2, macrophages, and endothelial cells, exhibiting strong connections (Figure 6A–C). In the COPD samples, they are closely associated with macrophages, monocytes/neutrophils, and pDCs. The significant activation signals between these cells are mainly related to antigen presentation (Figure 6D–F). Additionally, we observed that compared to the control group samples, the IL1B-(IL1R1+IL1RAP) signaling between cDCs and AT2 cells was significantly enhanced in COPD samples, the ANXA1-FRR1/FRR2 signaling between cDCs and macrophages was significantly enhanced, the HLA-A-CD8A/B, HLA-B-CD8A/B, and HLA-C-CD8A/B signaling between cDCs and T cells was enhanced, and the expression of HLA-D region genes between cDCs and pDCs was significantly enhanced in COPD samples (Figure 7A and B).

GSE26296 Differential Expression Analysis and Functional Enrichment

Utilizing the expression matrix data from mDCs obtained from lung tissues of individuals suffering from emphysema as well as control subjects, an analysis of differential expression was performed, uncovering a total of 656 genes that exhibited significant differences in expression. Among these, 332 genes exhibited upregulated expression levels, while 324 genes displayed downregulated expression levels (Figure 8A). GO analysis of these differentially expressed genes revealed their primary involvement in fatty acid metabolic processes, immune response cell activation, cellular lipid catabolic processes, and response to interferon-gamma. The external surfaces of the plasma membrane, vacuolar membrane, and secretory granule membrane were identified as the primary locations for the enrichment of these genes concerning cellular components. Furthermore, amide binding and peptide binding emerged as the predominant molecular functions in which these genes were enriched (Figure 8B). Furthermore, we performed KEGG enrichment analysis on the genes exhibiting differential expression. The findings indicated that genes with heightened expression were notably connected to anticoagulant resistance, the TNF signaling pathway, and the IL-17 signaling pathway. In contrast, the downregulated genes were mainly associated with complement and coagulation cascades, as well as the NOD-like receptor signaling pathway (Figure 8C and D).

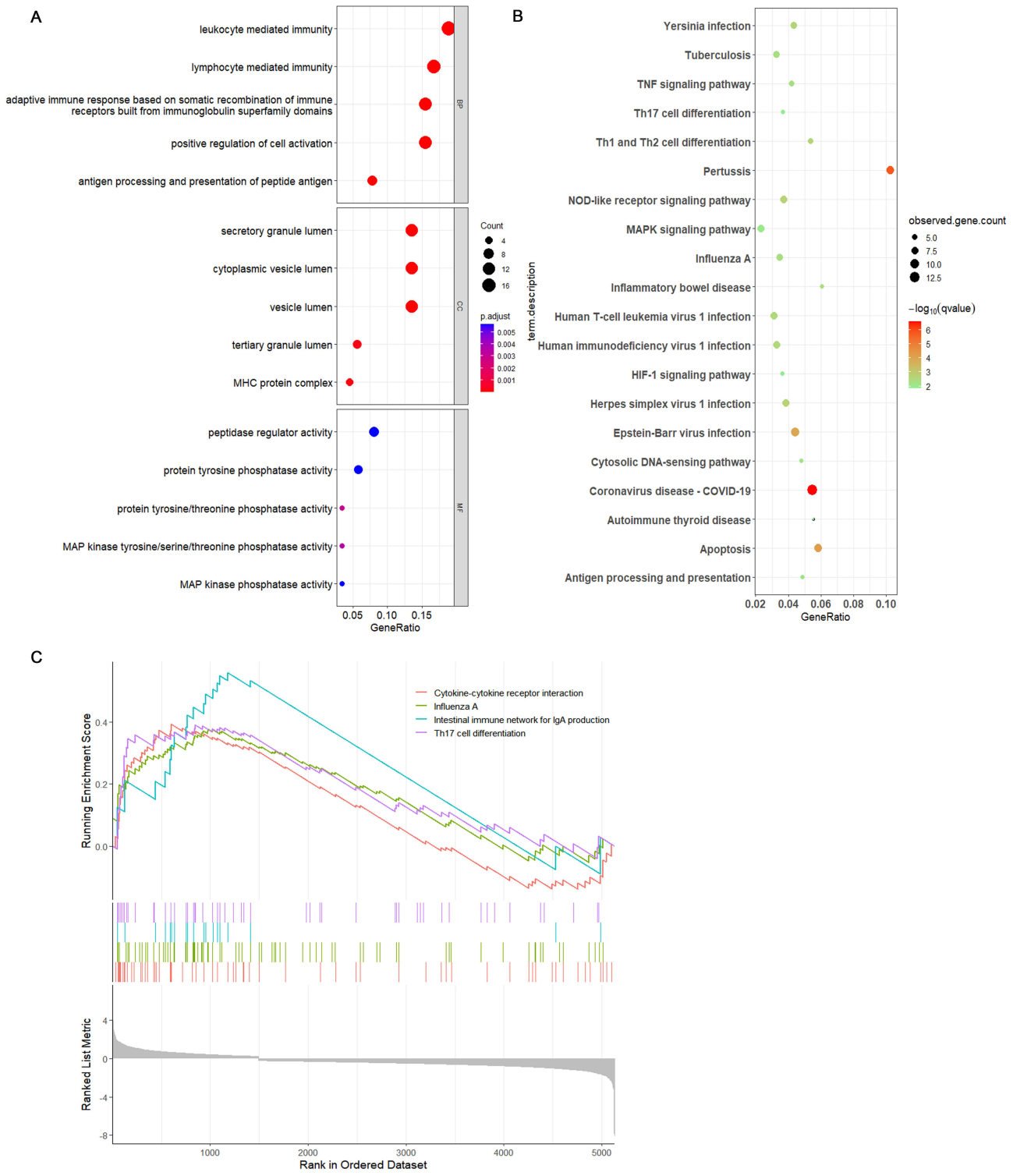

Figure 4 Enrichment analyses of DEGs in cDCs from scRNA-seq GSE196638. (**A**) GO enrichment analysis of DEGs in cDCs. (**B**) KEGG enrichment analysis of DEGs in cDCs. (**C**) GSEA enrichment analysis of DEGs in cDCs.

GSE38974 Weighted Gene Co-Expression Network Analysis and Differential Expression Analysis

The dataset underwent WGCNA to construct a sample clustering tree, which demonstrated robust sample clustering without any outlier samples (Figure 9A). Through the assessment of the scale-free fit index and the average connectivity at different

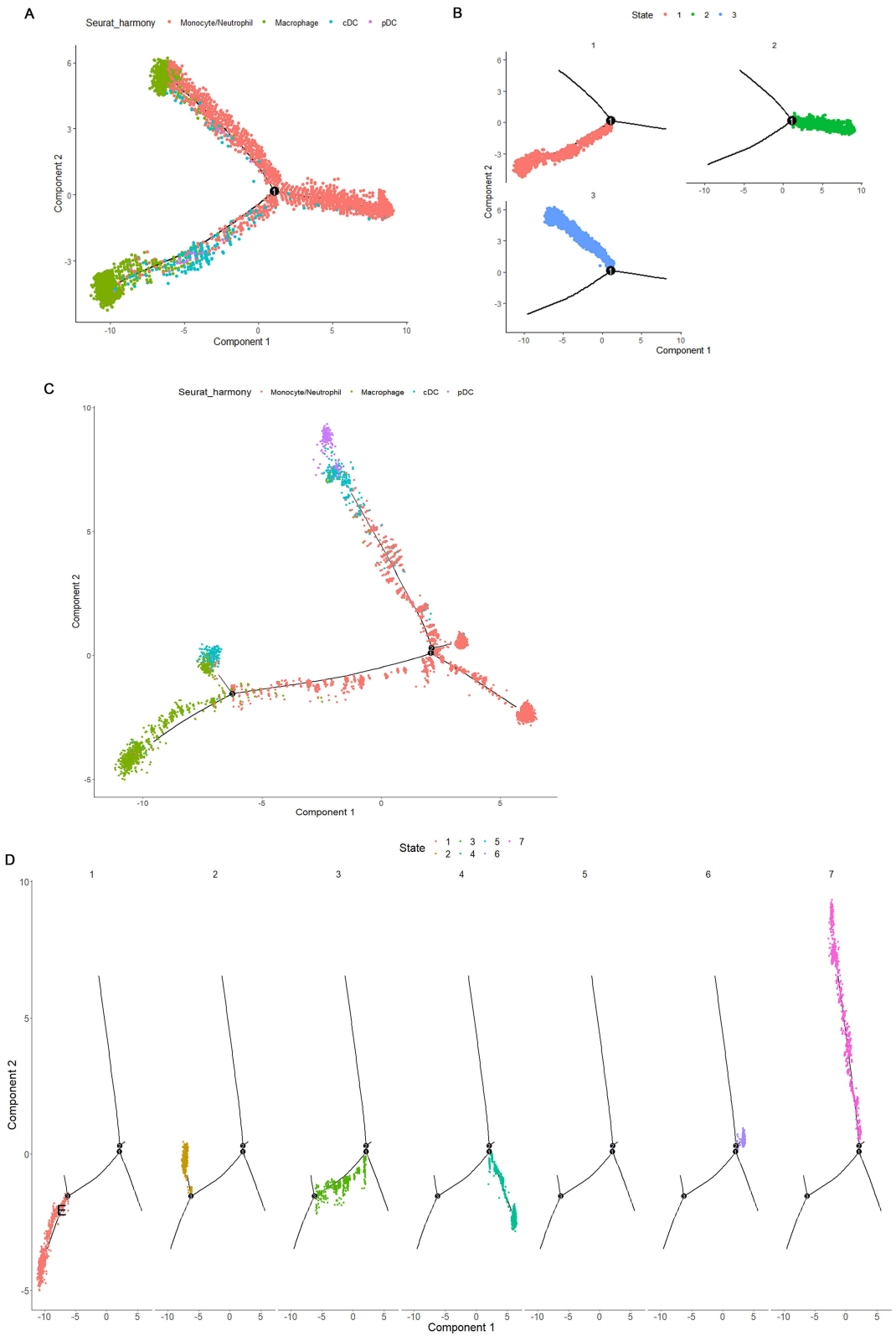

Figure 5 Trajectory analysis of myeloid cells in control and COPD samples. (**A** and **B**) Trajectory analysis focusing on myeloid cells from control samples. (**C** and **D**) Trajectory analysis focusing on myeloid cells from COPD samples.

https://doi.org/10.2147/COPD.S543753

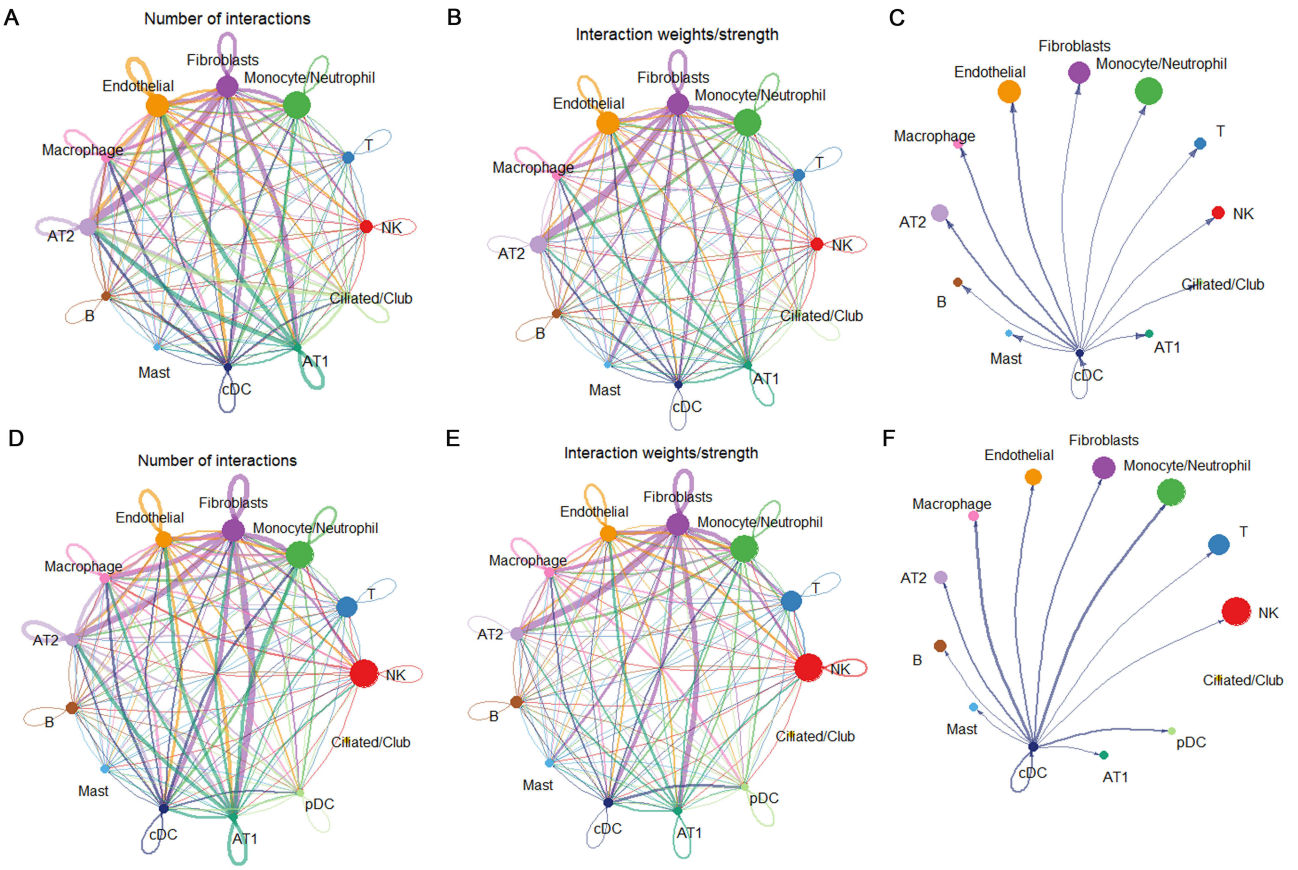

Figure 6 Analysis of cell-cell communication in single-cell samples. (**A** and **B**) Quantification and intensity of communication between cell clusters in control samples. (**C**) Strength of communication between cDCs and other cell clusters in control samples. (**D** and **E**) Number and strength of communication between cell clusters in COPD samples. (**F**) Strength of communication between cDCs and other cell clusters in COPD samples.

thresholds, it was concluded that a soft threshold of 8 is ideal for the construction of the network that follows (Figure 9B). Genes were clustered employing hierarchical clustering methods, and based on their co-expression characteristics, these genes were categorized into 15 distinct modules (Figure 9C). Correlation analyses between modules and traits related to COPD indicated that both the green-yellow and red modules were significantly associated with COPD ($p < 0.001$, $r = 0.92$; $p < 0.001$, $r = 0.75$) (Figure 9D). Furthermore, the correlation of the green-yellow and red modules with specific genes was calculated ($p < 0.001$, $cor = 0.92$; $p < 0.001$, $cor = 0.77$) (Figure 9E and F). Consequently, the genes within the green-yellow and red modules were identified as key genes associated with COPD for further analysis. Differential analysis of GSE38974 identified 1209 upregulated and 2085 downregulated differentially expressed genes. The analysis of GO enrichment for these genes primarily emphasized leukocyte migration along with the homeostasis of cellular divalent inorganic cations. These genes were largely enriched within the cellular components associated with cell-substrate junctions and the collagen-containing extracellular matrix. Regarding molecular function, they exhibited significant enrichment in cadherin binding and constituents that are structural components of the extracellular matrix (Figure 10A). Furthermore, the KEGG analysis uncovered several pathways, such as the interaction between cytokines and their receptors, the NF-kB signaling pathway, the IL-17 signaling pathway, the TNF signaling pathway, the Toll-like receptor signaling pathway, and the JAK-STAT signaling pathway (Figure 10B).

Identification of Common Differentially Expressed Genes

The results of differentially expressed gene analysis of GSE196638 cDCs, GSE26296 mDCs, GSE38974, and WGCNA module genes were compared and intersected. This analysis revealed one upregulated characteristic gene (RASGRP3) and three downregulated characteristic genes (C1QB, BLOC1S2, VSIG4) that were shared among the four groups (Figure 11A and B). Utilizing the expression data from the GSE38974 dataset for these genes, we developed ROC curves that link gene expression to

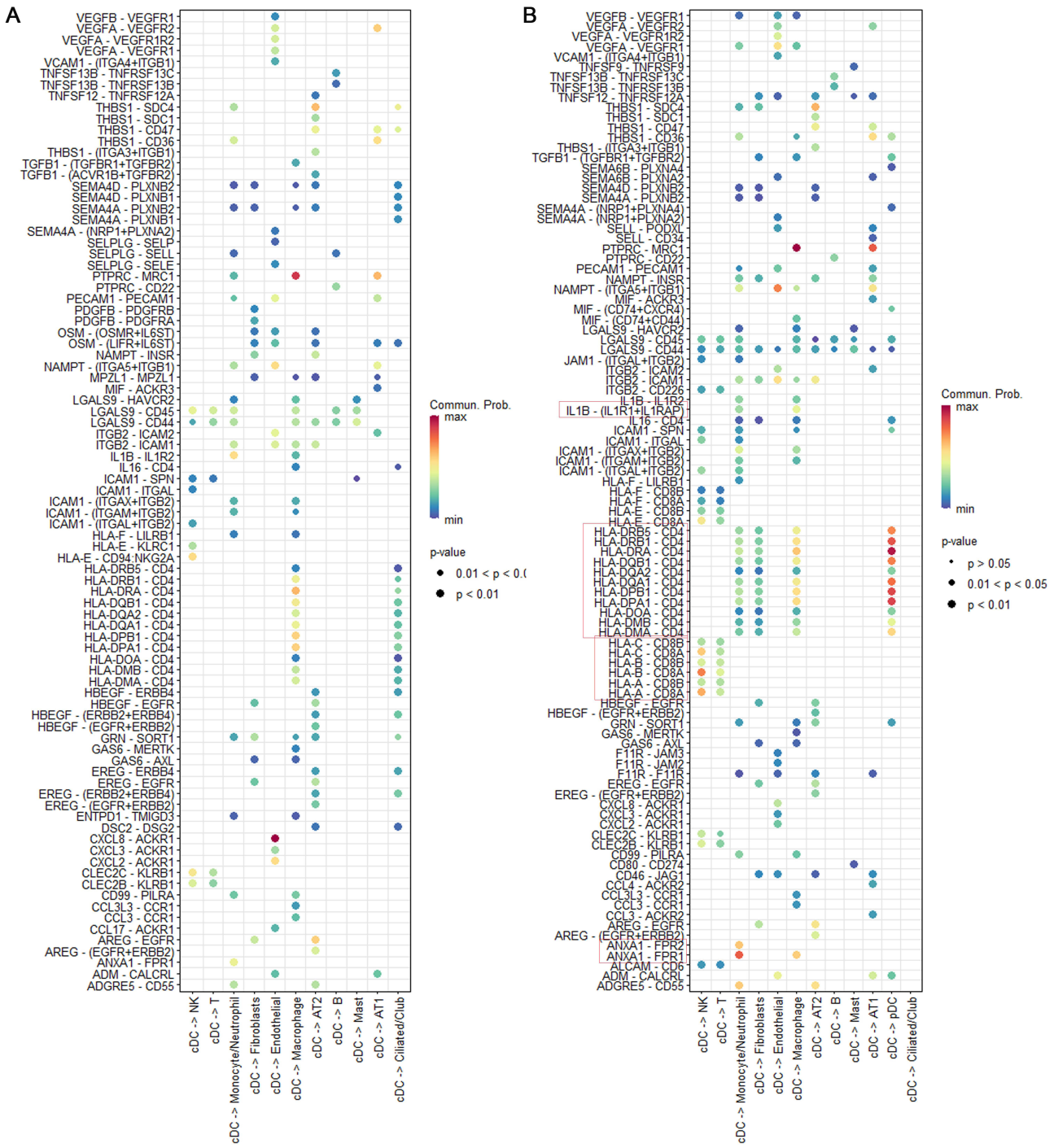

Figure 7 Cell–cell communication: Control vs COPD. (**A**) Bubble plot of cell-cell communication in control samples. (**B**) Bubble plot of cell-cell communication in COPD samples.

disease status. The AUC values were found to be 0.7866 for RASGRP3, 0.7413 for C1QB, 0.8889 for BLOC1S2, and 0.7988 for VSIG4, indicating that these genes exhibit significant diagnostic capability for the disease (Figure 11C–F).

Experimental Validation of Common Differentially Expressed Genes

H &E-stained lung sections showed CS-exposed mice had dilated alveolar spaces and a higher MLI than controls (Figure 12A and B). The results of RT-qPCR conducted on lung tissue from mice showed an elevated mRNA expression

https://doi.org/10.2147/COPD.S543753

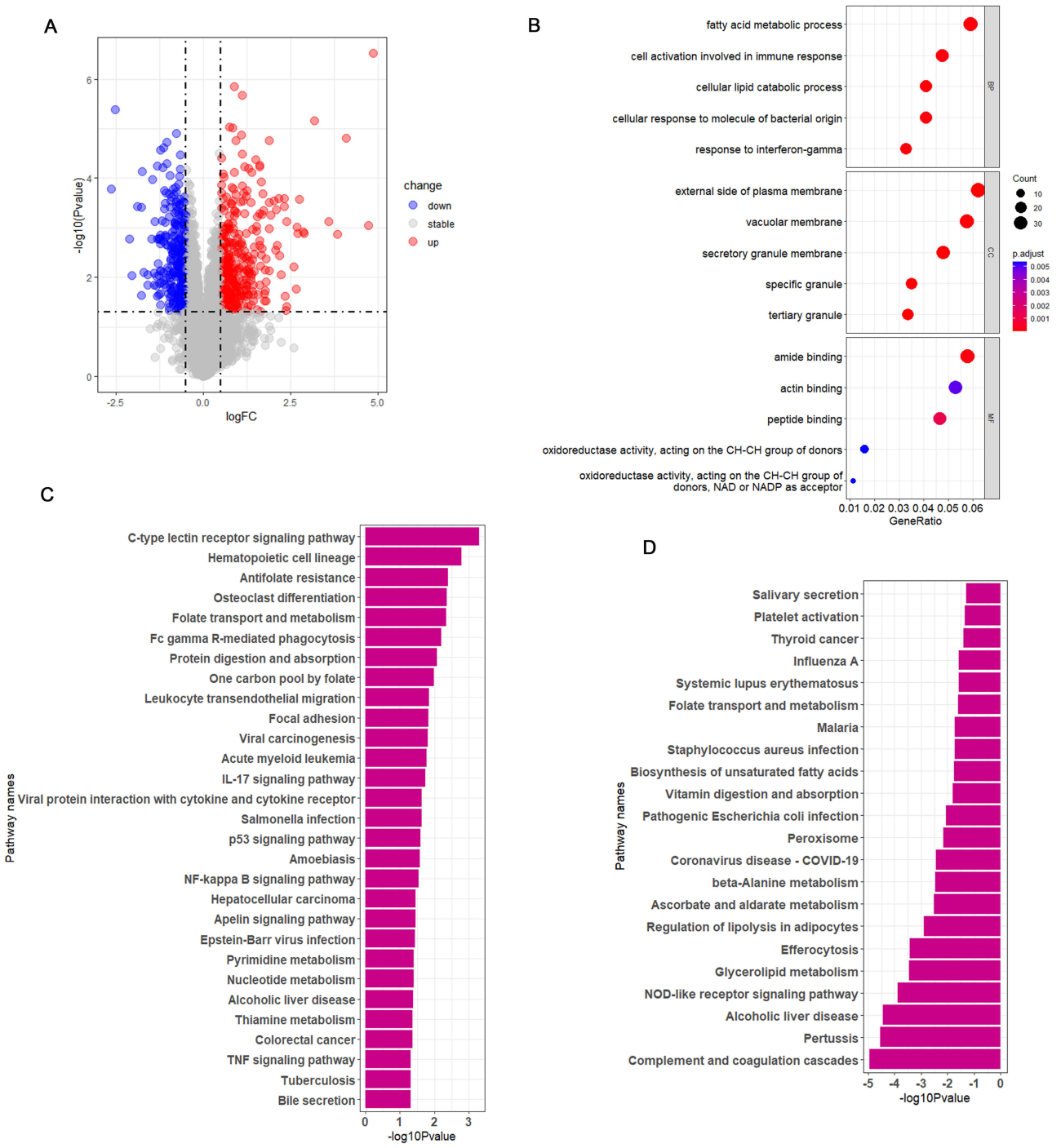

Figure 8 GSE26696 differential analysis volcano plot and GO, KEGG enrichment analysis. (**A**) Volcano plot. (**B**) GO enrichment analysis. (**C**) KEGG enrichment assessment for genes that are upregulated. (**D**) KEGG enrichment analysis for downregulated genes.

of RASGRP3 in the CS cohort, whereas the expression levels of C1QB, BLOC1S2, and VSIG4 were reduced (Figure 12C). We chose VSIG4 for subsequent validation via Western Blot (WB), which indicated a reduction in its protein expression in the lung tissue of the CS cohort compared to the control group (Figure 12D and E). Furthermore, RT-qPCR assessments indicated an increase in RASGRP3 mRNA levels in BMDCs exposed to CSE, while the levels of C1QB, BLOC1S2, and VSIG4 mRNA were found to be lower (Figure 12F). These results are consistent with those from the bioinformatics analysis conducted.

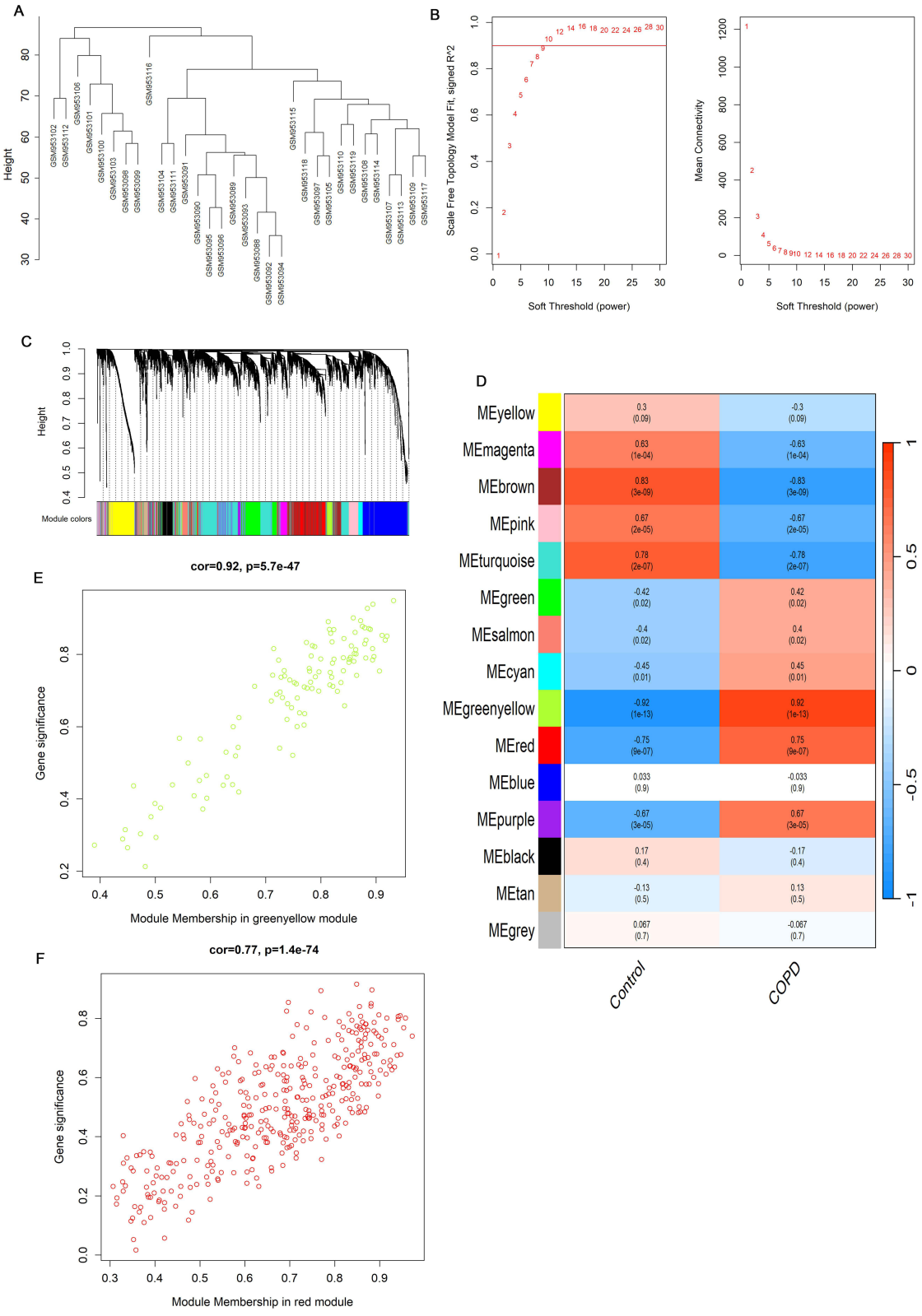

Figure 9 WGCNA analysis of the GSE38974 dataset. (**A**) Sample hierarchical clustering to detect outliers. No outliers were found, and all clusters were selected for subsequent analysis. (**B**) Construction of a scale-free co-expression network, selection of the optimal soft threshold power, with a threshold of 8. (**C**) Gene clustering dendrogram based on the dissimilarity measure (1-TOM). (**D**) Correlation between module eigengenes and disease phenotypes. (**E**) Scatter plot of module membership versus gene significance for the green-yellow module. (**F**) Scatter plot of module membership versus gene significance for the red module.

https://doi.org/10.2147/COPD.S543753

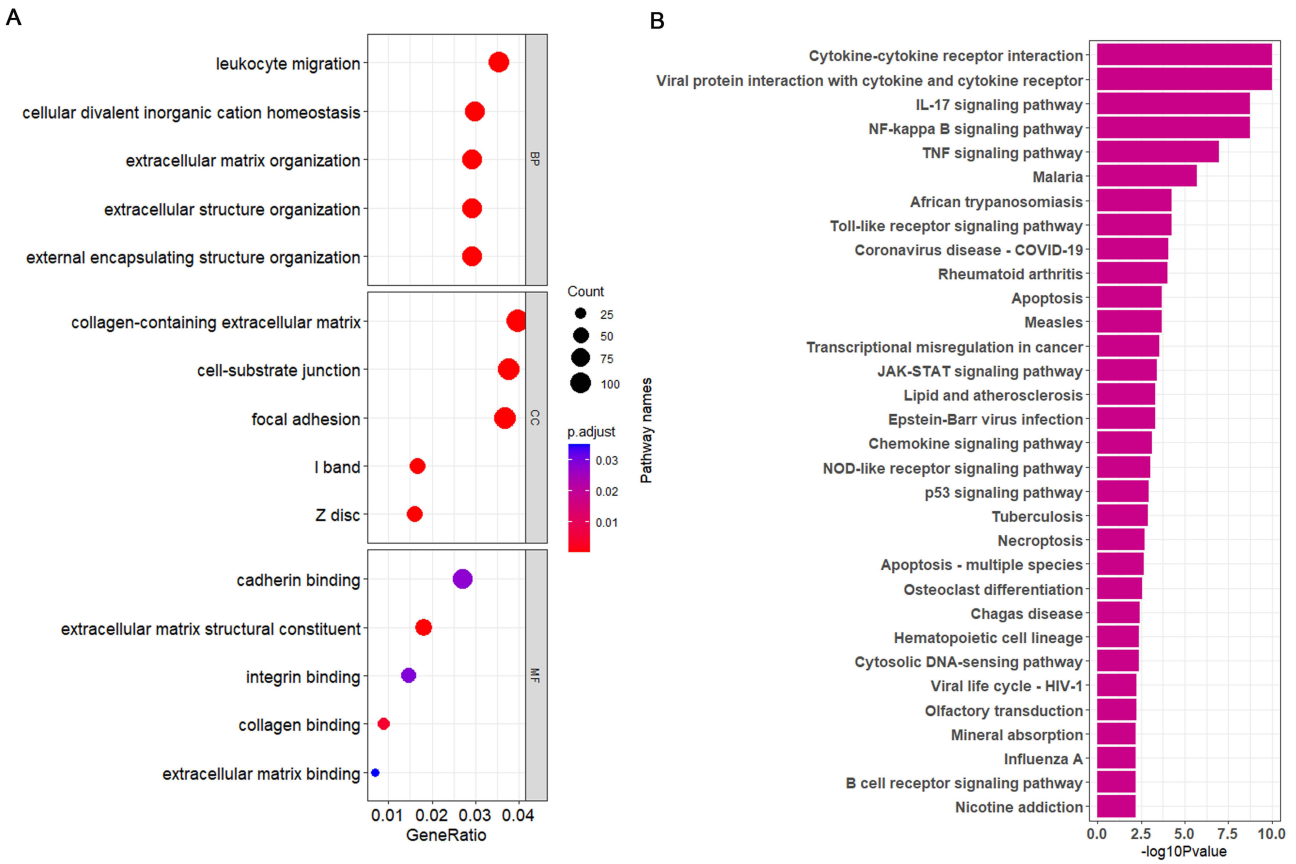

Figure 10 GO and KEGG enrichment of DEGs (GSE38974). (**A**) GO enrichment analysis. (**B**) KEGG enrichment analysis.

Discussion

The main pathological characteristics of COPD mainly consist of ongoing airway blockage, damage to lung tissue, and extended inflammatory reactions in the lungs. The prevalence and mortality rates associated with this disease have significantly increased on a global scale. Its pathogenesis is closely linked to the abnormal expression of various immune-related cytokines and inflammatory regulatory substances. As research into the immune regulatory mechanisms of COPD progresses within the medical community, novel treatment strategies based on immunomodulatory principles have gradually emerged as a significant focus in the field of COPD management.[42] DCs are crucial in the pathophysiology associated with chronic inflammation in COPD, playing a significant part in both the onset of the condition and its ongoing presence during the disease progression. Therefore, identifying genes associated with dendritic cells in COPD is essential for elucidating the disease's pathogenesis and developing targeted immunotherapies.

This research performed an in-depth examination of scRNA-seq and RNA-seq datasets to pinpoint four genes specific to DCs that are linked to COPD. To evaluate the diagnostic significance of these genes, ROC curves were created. RT-qPCR then quantified RASGRP3, C1QB, BLOC1S2 and VSIG4 mRNA in lungs of CS-induced emphysema mice and in CSE-treated BMDCs, while Western blot assessed VSIG4 protein in the lung tissue. This research effectively combined multi-omics data analysis with experimental validation to uncover a group of essential genes involved in the development of COPD that are vital in the regulation of dendritic cell activities. The results not only deepen our comprehension of the immune regulatory processes associated with COPD but also emphasize possible therapeutic targets for creating immunotherapy strategies centered on dendritic cells.

DCs are antigen-presenting cells that perform multiple immune regulatory functions. Compared to macrophages, DCs display a more robust capability to present antigens to B and T cells, thereby establishing a link between adaptive and innate immunity.[43] This research involved scRNA-seq examination of lung tissues obtained from both control and COPD groups,

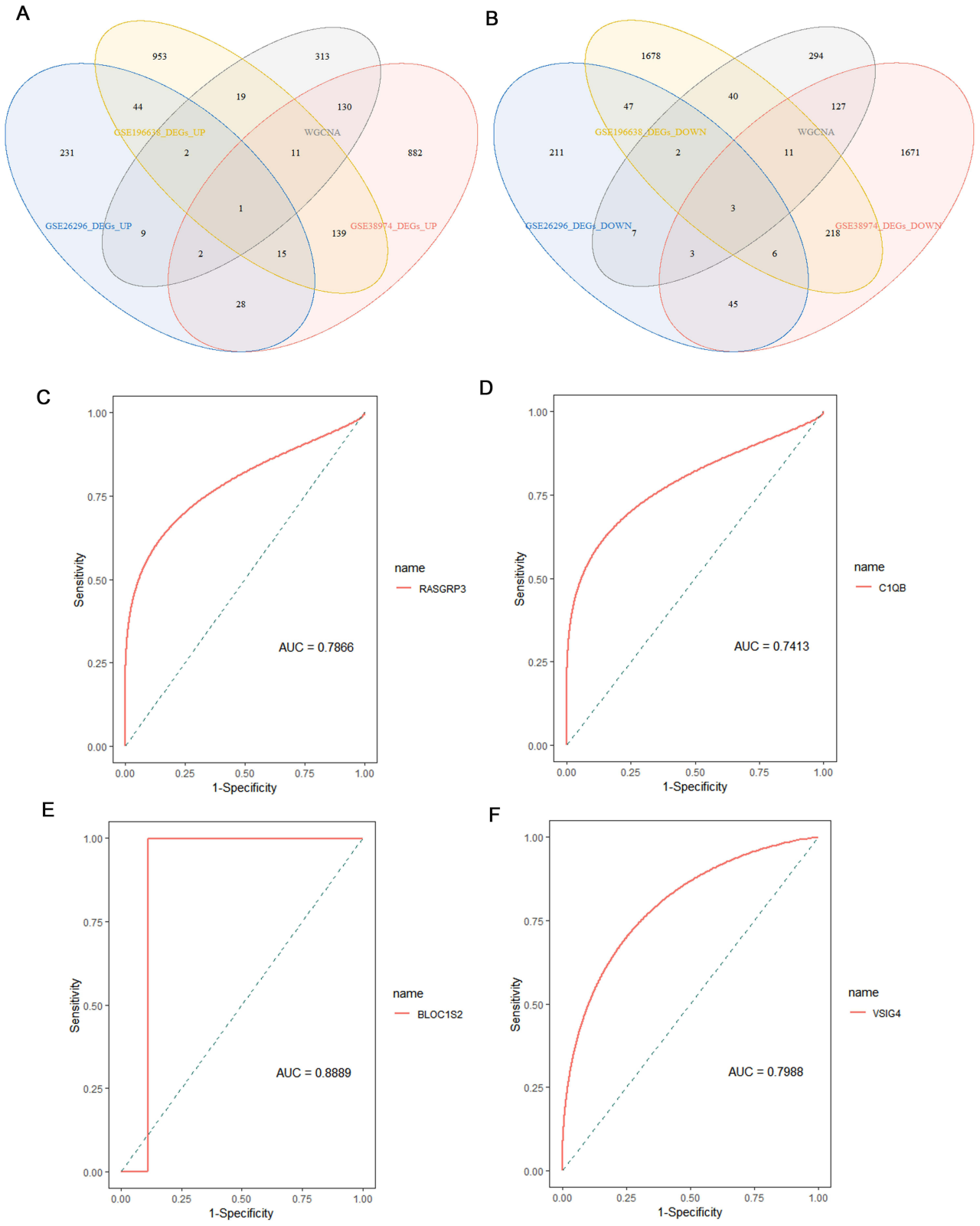

Figure 11 Identification of commonly differentially expressed genes and evaluation of predictive performance by calculating ROC curves in the GSE38974 dataset. (**A** and **B**) Intersection of differentially expressed genes in cDCs from GSE196638, in mDCs from GSE26296, in GSE38974, and WGCNA module genes. (**C**–**F**) Evaluation of predictive performance by calculating ROC curves and AUC values for the intersection genes in the GSE38974 dataset.

https://doi.org/10.2147/COPD.S543753

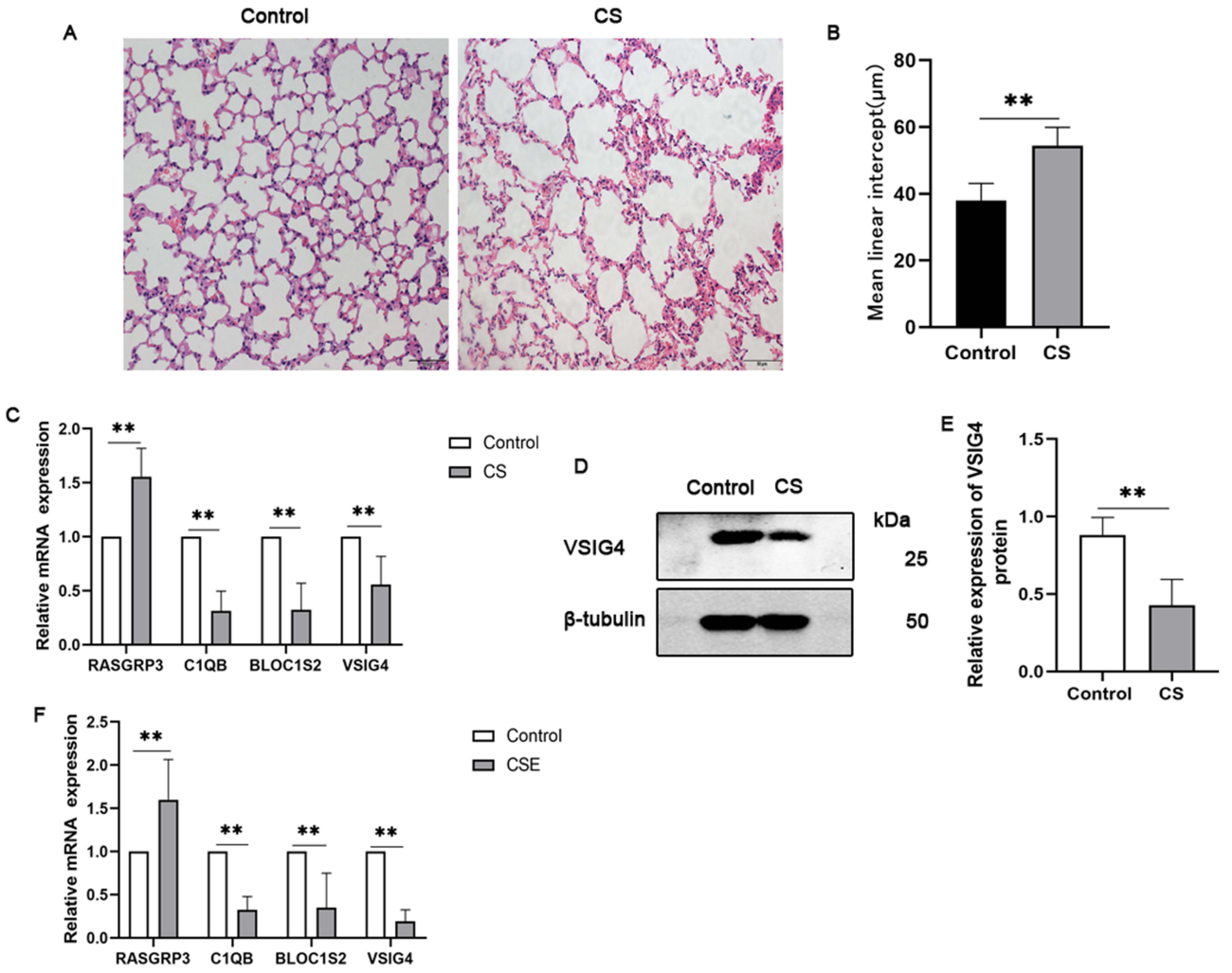

Figure 12 Experimental validation of differentially expressed genes. (**A**) Representative H&E-stained lung sections (scale bar, 50 μm). (**B**) MLI quantification (n=6). (**C**) RT-qPCR analysis of target genes in lung tissue (n=6). (**D** and **E**) Western-blot image (**D**) and quantification (**E**) of VSIG4 protein in lung tissue (n=6). (**F**) RT-qPCR of target genes in CSE-treated BMDCs (n=5). $*P < 0.05$, $**P < 0.01$, $***P < 0.001$, $****P < 0.0001$.

which demonstrated a notable increase and enhancement of pathways related to inflammatory responses in the DCs of individuals with COPD. The trajectory analysis indicated that the developmental pathway of myeloid cells in COPD patients is more complex. While cDCs emerged in the early developmental stages in both groups, a higher concentration of late-stage cDCs and pDCs was exclusively observed in the COPD group. The changes in dendritic cell states during COPD progression may correlate with disease advancement. Research has shown that during COPD development, the abnormal activation and infiltration of dendritic cells are positively correlated with disease severity and the exacerbation of inflammation.[44] Communication analysis revealed enhanced interactions between cDCs and macrophages, monocytes/neutrophils, and pDCs in COPD samples. The interactions between these cells are crucial in enhancing and speeding up the inflammatory response associated with COPD.[12,45–47] Improving these interactions could be vital in the inflammatory response and the advancement of COPD-related diseases.

The signaling of HLA-A-CD8A/B, HLA-B-CD8A/B, and HLA-C-CD8A/B between cDCs and T cells is significantly enhanced. cDCs present antigenic peptides through their HLA-A, HLA-B, and HLA-C surface molecules, while CD8+ T cells recognize these molecules via their CD8A and CD8B surface molecules. This improved interaction promotes the growth and specialization of T cells. Additionally, there is a significant rise in the expression of HLA-D region genes observed in cDCs and pDCs from samples taken from individuals with COPD, potentially aiding in the swift activation of CD4+ T cells. Our earlier research demonstrated that the levels of Th1 and Th17 cells are elevated in individuals with COPD as well as in mice suffering

from emphysema caused by CS. This imbalance between Th1 and Th17 cells contributes to the ongoing and worsening pulmonary inflammation associated with COPD.[37,48,49] In COPD patients, serum levels of IFN-γ and the supernatant of LPS-stimulated alveolar macrophages are elevated, leading to the upregulation of TLR2 and TLR4 expression in alveolar macrophages, thereby exacerbating the inflammatory response. Additionally, IFN-γ-induced STAT-1 signaling represents one of the mechanisms through which alveolar macrophages develop corticosteroid resistance, complicating anti-inflammatory treatment in COPD.[50,51] In the enrichment analysis, we noted a marked increase in the activity of inflammatory pathways. These include responses to interferon-gamma, differentiation of Th1/Th17 cells, as well as IL-17 and TNF signaling pathways, all of which are essential in the context of pulmonary inflammation. The unusual activation of these signaling pathways could result in an overproduction of inflammatory mediators, which in turn may cause ongoing inflammation in lung tissue and impair pulmonary function. These observations highlight the crucial importance of DCs within the immune microenvironment associated with COPD.

This study identified an elevated expression of RASGRP3 in dendritic cells within lung tissues from patients with COPD, suggesting its potential involvement in the development of emphysema. RASGRP3 is essential for processes such as cell growth, differentiation, and immune responses by activating the Ras-MAPK signaling pathway. During the initial phases of T cell maturation, it has a crucial function and additionally influences B cell growth by enhancing Ras signaling through the B cell receptor.[52,53] In the past few years, there has been a growing interest in the function of RASGRP3 concerning lung diseases, particularly noting its amplification in cases of lung cancer.[54] Nevertheless, the precise contribution of RASGRP3 to the progression of COPD is still not well understood. Our research indicates that RASGRP3 is elevated in DCs derived from lung tissue samples of individuals suffering from COPD. Our experiments further demonstrated an upregulation of RASGRP3 in both CSE-treated BMDCs and lung tissues of CS-induced emphysema mice. RASGRP3 could play a role in the inflammatory response by regulating the development and activity of DCs, which in turn impacts their ability to present antigens.

C1QB, BLOC1S2, and VSIG4, identified as downregulated signature genes, may contribute to the development of COPD through the loss or inhibition of their functions. C1QB, the β subunit of complement C1q, is a crucial component of the classical complement pathway and plays a significant role in immune regulation and inflammatory responses. Stimulation by CS leads to a reduction in C1q levels, thereby promoting emphysema. The downregulation of C1q expression in lung CD1a+ antigen-presenting cells isolated from emphysema patients and from mice with CS-induced emphysema results in an increase in Th17 cells, which amplifies pulmonary inflammation.[55] BLOC1S2 is involved in lysosome biogenesis and transport.[56] In patients with COPD, the lung tissues and pulmonary epithelium exhibit abnormal activation of autophagy, which results in the degradation of lysosomes.[57] Individuals diagnosed with Parkinson's disease receiving nicotinamide riboside supplementation show heightened levels of BLOC1S2 expression in peripheral blood mononuclear cells, subsequently leading to a reduction in inflammatory cytokine levels.[58] In addition, BLOC1S2 regulates the growth and maturation of hepatic stellate cells. Moreover, fetal liver hematopoietic stem cells that do not express BLOC1S2 exhibit deficiencies in both lymphoid and myeloid differentiation.[59] The specific role of BLOC1S2 in pulmonary diseases has yet to be elucidated. Our research revealed that the levels of expression for C1QB and BLOC1S2 in DCs obtained from the lung tissues of patients with COPD are notably reduced. Additionally, experimental validation revealed reduced expression of C1QB and BLOC1S2 in both CSE-treated BMDCs and lung tissues of CS-induced emphysema mice. While the candidate gene BLOC1S2 exhibited the highest AUC in our receiver operating characteristic (ROC) assessment, it was not selected for validation because experimental reports concerning immune regulation were lacking in databases such as UniProt, ImmPort, and PubMed. In contrast, VSIG4 provides more direct evidence related to immune regulation. Recognized as a restrictive immune checkpoint receptor, VSIG4's expression has been documented on conventional dendritic cells type 2 (cDC2) and macrophages, where it acts to inhibit T cell proliferation as well as the secretion of IL-2 and IFN-γ. Belonging to the B7 family, VSIG4 (V-set immunoglobulin domain-containing protein 4) is primarily found on the surfaces of macrophages and dendritic cells in the immune system. Research has demonstrated that this immunoregulatory molecule is essential for maintaining immune homeostasis. In the pathological context of COPD, the expression level of VSIG4 in alveolar macrophages is significantly diminished, which inhibits its anti-inflammatory function and contributes to the progression of COPD.[60] Co-culturing 293FT cells with increased expression of VSIG4 with CD8+ T cells results in reduced proliferation as well as decreased secretion of cytokines such as IL-2 and

IFN-γ in lung cancer.[61] Experiments revealed a reduction in VSIG4 expression in CSE-exposed BMDCs and lung tissues from CS-induced emphysema mice, with protein levels confirmed by Western blot. Based on bioinformatics data, it is hypothesized that this phenomenon may stimulate the proliferation and activation of CD8+ T cells and CD4+ T cells, thereby inhibiting anti-inflammatory effects and enhancing the inflammatory response. The evaluation results of the ROC curve indicate that the four intersecting genes possess high accuracy in diagnosing COPD and may serve as potential diagnostic markers. Additionally, the results of the study indicate a strong connection between RASGRP3, C1QB, BLOC1S2, and VSIG4 and the inflammatory processes occurring in DCs. However, the precise mechanisms by which these factors influence inflammation in DCs related to COPD require more in-depth exploration.

This research has uncovered important insights related to the immune response linked to COPD. While our study provides valuable insights, it is crucial to acknowledge some inherent limitations. A key limitation is the absence of clinical samples to clarify how these genes drive COPD onset and progression in DCs. Additionally, interactions with other immune cells require further experimental verification to elucidate their potential immune mechanisms. Despite these limitations, our study may provide new targets for addressing dendritic cell inflammation in COPD and offer fresh insights and theoretical foundations for future in-depth research.

Conclusion

To summarize, integrating scRNA-seq/RNA-seq and experimental validation, we identified four DC-linked genes (RASGRP3, C1QB, BLOC1S2 and VSIG4) in COPD lung tissue that can serve as early diagnostic biomarkers and provide therapeutic targets for precision therapy for COPD, while also offering new insights into DC-driven inflammation mechanisms.

Institutional Review Board Statement

All human datasets (GSE196638, GSE26296 and GSE38974) are publicly available and de-identified. The Medical Ethics Committee of the First Affiliated Hospital of Guangxi Medical University formally reviewed and approved this research (Approval No. 2025-E0752) in accordance with the Declaration of Helsinki and institutional guidelines for secondary use of human data. The animal study protocol was approved by the Guangxi Medical University Laboratory Animal Committee (No.202503381).

Data Sharing Statement

If original data were required, the corresponding author was contacted. We are glad to provide the original data or add them to the attachment.

Funding

This study was supported by the National Natural Science Foundation of China (82260009).

Disclosure

The authors declare no conflicts of interest.

References

1. Wang C, Xu J, Yang L, et al. Prevalence and risk factors of chronic obstructive pulmonary disease in China (the China pulmonary health [CPH] study): a national cross-sectional study. *Lancet*. 2018;391(10131):1706–1717. doi:10.1016/S0140-6736(18)30841-9
2. Cosio MG, Saetta M, Agusti A.Immunologic aspects of chronic obstructive pulmonary disease. *N Engl J Med*. 2009;360(23):2445–2454. doi:10.1056/NEJMra0804752
3. Verleden SE, Hendriks JMH, Snoeckx A, et al. Small airway disease in pre-chronic obstructive pulmonary disease with emphysema: a cross-sectional study. *Am J Respir Crit Care Med*. 2024;209(6):683–692. doi:10.1164/rccm.202301-0132OC
4. Shan M, Cheng HF, Song LZ, et al. Lung myeloid dendritic cells coordinately induce TH1 and TH17 responses in human emphysema. *Sci Transl Med*. 2009;1(4):4ra10. doi:10.1126/scitranlsmed.3000154
5. Yin P, Wu J, Wang L, et al. The burden of COPD in China and its provinces: findings from the global burden of disease study 2019. *Front Public Health*. 2022;10:859499. doi:10.3389/fpubh.2022.859499

6. Safiri S, Carson-Chahhoud K, Noori M, et al. Burden of chronic obstructive pulmonary disease and its attributable risk factors in 204 countries and territories, 1990-2019: results from the global burden of disease study 2019. *BMJ*. 2022;378:e069679. doi:10.1136/bmj-2021-069679
7. Aono Y, Suzuki Y, Horiguchi R, et al. CD109 on dendritic cells regulates airway hyperreactivity and eosinophilic airway inflammation. *Am J Respir Cell Mol Biol*. 2023;68(2):201–212. doi:10.1165/rcmb.2022-0109OC
8. Iwasaki A, Medzhitov R. Control of adaptive immunity by the innate immune system. *Nat Immunol*. 2015;16(4):343–353. doi:10.1038/ni.3123
9. Guilliams M, Ginhoux F, Jakubzick C, et al. Dendritic cells, monocytes and macrophages: a unified nomenclature based on ontogeny. *Nat Rev Immunol*. 2014;14(8):571–578. doi:10.1038/nri3712
10. Freeman CM, Curtis JL. Lung dendritic cells: shaping immune responses throughout chronic obstructive pulmonary disease progression. *Am J Respir Cell Mol Biol*. 2017;56(2):152–159. doi:10.1165/rcmb.2016-0272TR
11. Demedts IK, Bracke KR, Van Pottelberge G, et al. Accumulation of dendritic cells and increased CCL20 levels in the airways of patients with chronic obstructive pulmonary disease. *Am J Respir Crit Care Med*. 2007;175(10):998–1005. doi:10.1164/rccm.200608-1113OC
12. Paplinska-Goryca M, Misiukiewicz-Stepien P, Nejman-Gryz P, et al. Epithelial-macrophage-dendritic cell interactions impact alarmins expression in asthma and COPD. *Clin Immunol*. 2020;215:108421. doi:10.1016/j.clim.2020.108421
13. Gianello V, Salvi V, Parola C, et al. The PDE4 inhibitor CHF6001 modulates pro-inflammatory cytokines, chemokines and Th1- and Th17-polarizing cytokines in human dendritic cells. *Biochem Pharmacol*. 2019;163:371–380. doi:10.1016/j.bcp.2019.03.006
14. Chen KY, Sun WL, Wu SM, et al. Reduced tolerogenic program death-ligand 1-expressing conventional type 1 dendritic cells are associated with rapid decline in chronic obstructive pulmonary disease. *Cells*. 2024;13(10):878. doi:10.3390/cells13100878
15. Le Rouzic O, Koné B, Kluza J, et al. Cigarette smoke alters the ability of human dendritic cells to promote anti-Streptococcus pneumoniae Th17 response. *Respir Res*. 2016;17(1):94. doi:10.1186/s12931-016-0408-6
16. Vassallo R, Walters PR, Lamont J, et al. Cigarette smoke promotes dendritic cell accumulation in COPD; a lung tissue research consortium study. *Respir Res*. 2010;11(1):45. doi:10.1186/1465-9921-11-45
17. Jia L, Li N, Abdelaal TRM, et al. High-dimensional mass cytometry reveals emphysema-associated changes in the pulmonary immune system. *Am J Respir Crit Care Med*. 2024;210(8):1002–1016. doi:10.1164/rccm.202303-0442OC
18. Pfeffer PE, Ho TR, Mann EH, et al. Urban particulate matter stimulation of human dendritic cells enhances priming of naive CD8 T lymphocytes. *Immunology*. 2018;153(4):502–512. doi:10.1111/imm.12852
19. Hodge S, Hodge G, Holmes M, et al. Increased CD8T -cell granzyme B in COPD is suppressed by treatment with low-dose azithromycin. *Respirology*. 2015;20(1):95–100. doi:10.1111/resp.12415
20. Givi ME, Redegeld FA, Folkerts G, et al. Dendritic cells in pathogenesis of COPD. *Curr Pharm Des*. 2012;18(16):2329–2335. doi:10.2174/138161212800166068
21. Upham JW, Xi Y. Dendritic cells in human lung disease: recent advances. *Chest*. 2017;151(3):668–673. doi:10.1016/j.chest.2016.09.030
22. Qiu SL, Sun QX, Zhou JP, et al. IL-27 mediates anti-inflammatory effect in cigarette smoke induced emphysema by negatively regulating IFN-γ producing cytotoxic CD8+ T cells in mice. *Eur J Immunol*. 2022;52(2):222–236. doi:10.1002/eji.202049076
23. Naessens T, Morias Y, Hamrud E, et al. Human lung conventional dendritic cells orchestrate lymphoid neogenesis during chronic obstructive pulmonary disease. *Am J Respir Crit Care Med*. 2020;202(4):535–548. doi:10.1164/rccm.201906-1123OC
24. Zheng H, Wang G, Wang Y, et al. Combined analysis of bulk RNA and single-cell RNA sequencing to identify pyroptosis-related markers and the role of dendritic cells in chronic obstructive pulmonary disease. *Heliyon*. 2024;10(6):e27808. doi:10.1016/j.heliyon.2024.e27808
25. Nakamizo S, Dutertre CA, Khalilnezhad A, et al. Single-cell analysis of human skin identifies CD14+ type 3 dendritic cells co-producing IL1B and IL23A in psoriasis. *J Exp Med*. 2021;218(9):e20202345. doi:10.1084/jem.20202345
26. Hao Y, Hao S, Andersen-Nissen E, et al. Integrated analysis of multimodal single-cell data. *Cell*. 2021;184(3):3573–87.e29. doi:10.1016/j.cell.2021.04.048
27. Ren YF, Ma Q, Zeng X, et al. Single-cell RNA sequencing reveals immune microenvironment niche transitions during the invasive and metastatic processes of ground-glass nodules and part-solid nodules in lung adenocarcinoma. *Mol Cancer*. 2024;23(1):263. doi:10.1186/s12943-024-02177-7
28. Zhang Y, Liu G, Zeng Q, et al. CCL19-producing fibroblasts promote tertiary lymphoid structure formation enhancing anti-tumor IgG response in colorectal cancer liver metastasis. *Cancer Cell*. 2024;42(8):1370–85.e9. doi:10.1016/j.ccell.2024.07.006
29. Becht E, McInnes L, Healy J, et al. Dimensionality reduction for visualizing single-cell data using UMAP. *Nat Biotechnol*. 2018. doi:10.1038/nbt.4314
30. Qiu X, Mao Q, Tang Y, et al. Reversed graph embedding resolves complex single-cell trajectories. *Nat Methods*. 2017;14(10):979–982. doi:10.1038/nmeth.4402
31. Ritchie ME, Phipson B, Wu D, et al. limma powers differential expression analyses for RNA-sequencing and microarray studies. *Nucleic Acids Res*. 2015;43(7):e47. doi:10.1093/nar/gkv007
32. Wu T, Hu E, Xu S, et al. clusterProfiler 4.0: a universal enrichment tool for interpreting omics data. *Innovation*. 2021;2(3):100141. doi:10.1016/j.xinn.2021.100141
33. Kanehisa M, Goto S. KEGG: kyoto encyclopedia of genes and genomes. *Nucleic Acids Res*. 2000;28(1):27–30. doi:10.1093/nar/28.1.27
34. Kanehisa M, Furumichi M, Sato Y, et al. KEGG for taxonomy-based analysis of pathways and genomes. *Nucleic Acids Res*. 2023;51(D1):D587–D92. doi:10.1093/nar/gkac963
35. Zhang B, Horvath S. A general framework for weighted gene co-expression network analysis. *Stat Appl Genet Mol Biol*. 2005;4(1):Article17. doi:10.2202/1544-6115.1128
36. Langfelder P, Horvath S. WGCNA: an R package for weighted correlation network analysis. *BMC Bioinf*. 2008;9(559):559. doi:10.1186/1471-2105-9-559
37. Qiu S, Zhou G, Ke J, et al. Impairment of Gal-9 and Tim-3 crosstalk between Tregs and Th17 cells drives tobacco smoke-induced airway inflammation. *Immunology*. 2024;173(1):152–171. doi:10.1111/imm.13820
38. Zheng G, Li C, Chen X, et al. HDAC9 inhibition reduces skeletal muscle atrophy and enhances regeneration in mice with cigarette smoke-induced COPD. *Biochim Biophys Acta Mol Basis Dis*. 2024;1870(3):167023. doi:10.1016/j.bbadis.2024.167023
39. Li C, Deng Z, Zheng G, et al. Resveratrol prevents skeletal muscle atrophy and senescence via regulation of histone deacetylase 2 in cigarette smoke-induced mice with emphysema. *J Inflamm Res*. 2022;15:5425–5437. doi:10.2147/JIR.S383180

40. Nii T, Maeda Y, Motooka D, et al. Genomic repertoires linked with pathogenic potency of arthritogenic Prevotella copri isolated from the gut of patients with rheumatoid arthritis. *Ann Rheum Dis*. 2023;82(5):621–629. doi:10.1136/ard-2022-222881
41. Fu W, Li X, Li Y, et al. A programmable releasing versatile hydrogel platform boosts systemic immune responses via sculpting tumor immunogenicity and reversing tolerogenic dendritic cells. *Biomaterials*. 2024;305:122444. doi:10.1016/j.biomaterials.2023.122444
42. Kheradmand F, Zhang Y, Corry DB.Contribution of adaptive immunity to human COPD and experimental models of emphysema. *Physiol Rev*. 2023;103(2):1059–1093. doi:10.1152/physrev.00036.2021
43. Hinshaw DC, Shevde LA. The tumor microenvironment innately modulates cancer progression. *Cancer Res*. 2019;79(18):4557–4566. doi:10.1158/0008-5472.CAN-18-3962
44. Zanini A, Spanevello A, Baraldo S, et al. Decreased maturation of dendritic cells in the central airways of COPD patients is associated with VEGF, TGF-β and vascularity. *Respiration*. 2014;87(3):234–242. doi:10.1159/000356749
45. Paplinska-Goryca M, Misiukiewicz-Stepien P, Proboszcz M, et al. Interactions of nasal epithelium with macrophages and dendritic cells variously alter urban PM-induced inflammation in healthy, asthma and COPD. *Sci Rep*. 2021;11(1):13259. doi:10.1038/s41598-021-92626-w
46. Chen J, Wang T, Li X, et al. DNA of neutrophil extracellular traps promote NF-κB-dependent autoimmunity via cGAS/TLR9 in chronic obstructive pulmonary disease. *Signal Transduct Target Ther*. 2024;9(1):163. doi:10.1038/s41392-024-01881-6
47. Günes Günsel G, Conlon TM, Jeridi A, et al. The arginine methyltransferase PRMT7 promotes extravasation of monocytes resulting in tissue injury in COPD. *Nat Commun*. 2022;13(1):1303. doi:10.1038/s41467-022-28809-4
48. Qiu SL, Duan MC, Liang Y, et al. Cigarette smoke induction of interleukin-27/WSX-1 regulates the differentiation of Th1 and Th17 cells in a smoking mouse model of emphysema. *Front Immunol*. 2016;7:553. doi:10.3389/fimmu.2016.00553
49. Ke J, Huang S, He Z, et al. NFIL3/Tim3 axis regulates effector Th1 inflammation in COPD mice. *Front Immunol*. 2024;15:1482213. doi:10.3389/fimmu.2024.1482213
50. Gutiérrez-Romero KJ, Falfán-Valencia R, Ramírez-Venegas A, et al. Altered levels of IFN-γ, IL-4, and IL-5 depend on the TLR4 rs4986790 genotype in COPD smokers but not those exposed to biomass-burning smoke. *Front Immunol*. 2024;15:1411408. doi:10.3389/fimmu.2024.1411408
51. Southworth T, Metryka A, Lea S, et al. IFN-γ synergistically enhances LPS signalling in alveolar macrophages from COPD patients and controls by corticosteroid-resistant STAT1 activation. *Br J Pharmacol*. 2012;166(7):2070–2083. doi:10.1111/j.1476-5381.2012.01907.x
52. Golec DP, Henao Caviedes LM, Baldwin TA. Baldwin TA RasGRP1 and RasGRP3 are required for efficient generation of early thymic progenitors. *J Immunol*. 2016;197(5):1743–1753. doi:10.4049/jimmunol.1502107
53. Coughlin JJ, Stang SL, Dower NA, et al. RasGRP1 and RasGRP3 regulate B cell proliferation by facilitating B cell receptor-Ras signaling. *J Immunol*. 2005;175(11):7179–7184. doi:10.4049/jimmunol.175.11.7179
54. Nakachi I, Rice JL, Coldren CD, et al. Application of SNP microarrays to the genome-wide analysis of chromosomal instability in premalignant airway lesions. *Cancer Prev Res*. 2014;7(2):255–265. doi:10.1158/1940-6207.CAPR-12-0485
55. Yuan X, Chang CY, You R, et al. Cigarette smoke-induced reduction of C1q promotes emphysema. *JCI Insight*. 2019;5(13):e124317. doi:10.1172/jci.insight.124317
56. Zhou W, He Q, Zhang C, et al. BLOS2 negatively regulates Notch signaling during neural and hematopoietic stem and progenitor cell development. *Elife*. 2016;5:e18108. doi:10.7554/eLife.18108
57. Jeong YJ, Lee KH, Woo J, et al. Downregulation of lysosome-associated membrane protein-2A contributes to the pathogenesis of COPD. *Int J Chron Obstruct Pulmon Dis*. 2023;18:289–303. doi:10.2147/COPD.S378386
58. Brakedal B, Dölle C, Riemer F, et al. The NADPARK study: a randomized Phase I trial of nicotinamide riboside supplementation in Parkinson's disease. *Cell Metab*. 2022;34(3):396–407.e6. doi:10.1016/j.cmet.2022.02.001
59. He Q, Gao S, Lv J, et al. BLOS2 maintains hematopoietic stem cells in the fetal liver via repressing Notch signaling. *Exp Hematol*. 2017;51:1–6.e2. doi:10.1016/j.exphem.2017.03.002
60. Liu Y, Liu H, Li C, et al. Proteome profiling of lung tissues in chronic obstructive pulmonary disease (COPD): platelet and macrophage dysfunction contribute to the pathogenesis of COPD. *Int J Chron Obstruct Pulmon Dis*. 2020;15:973–980. doi:10.2147/COPD.S246845
61. Liao Y, Guo S, Chen Y, et al. VSIG4 expression on macrophages facilitates lung cancer development. *Lab Invest*. 2014;94(7):706–715. doi:10.1038/labinvest.2014.73